IEEE Access
Multidisciplinary | Rapid Review | Open Access Journal

IEEE ENGINEERING IN MEDICINE AND BIOLOGY SOCIETY SECTION

Received April 13, 2021, accepted May 11, 2021, date of publication May 26, 2021, date of current version June 8, 2021.

Digital Object Identifier 10.1109/ACCESS.2021.3083772

Intelligent Wireless EEG Measurement System With Electrical and Optogenetic Stimulation for Epileptic Seizure Detection and Suppression

WEI-EN LEE[1], (Member, IEEE), CHIEH TSOU[2], (Member, IEEE), ZHAN-XIAN LIAO[2], (Graduate Student Member, IEEE), PO-YEN LU[3], TSUNG-HSIEN LIN[1], (Senior Member, IEEE), SHUENN-YUH LEE[2], (Senior Member, IEEE), CHOU-CHING K. LIN[4], (Senior Member, IEEE), AND GIA-SHING SHIEH[5]

[1]Department of Electrical Engineering, National Taiwan University, Taipei 10617, Taiwan
[2]Department of Electrical Engineering, National Cheng Kung University, Tainan City 70101, Taiwan
[3]Department of Mechanical Engineering, National Cheng Kung University, Tainan City 70101, Taiwan
[4]Division of Neurology, National Cheng-Kung University Hospital, Tainan City 70101, Taiwan
[5]Division of Urology, Ministry of Health and Welfare Tainan Hospital, Tainan City 70101, Taiwan

Corresponding authors: Tsung-Hsien Lin (thlin@ntu.edu.tw) and Shuenn-Yuh Lee (ieesyl@mail.ncku.edu.tw)

This work was supported in part by the Taiwan Semiconductor Research Institute, and in part by the Ministry of Science and Technology (MOST), Taiwan, under Grant MOST 109-2221-E-002-138-MY2.

This work involved human subjects or animals in its research. Approval of all ethical and experimental procedures and protocols was granted by the Institutional Animal Care and Use Committee (IACUC).

ABSTRACT A two-channel real-time intelligent electroencephalography (EEG) measurement system with electrical and optical stimulations is presented for seizure detection and suppression. Based on software control through a wireless interface, this system provides closed- and open-loop feedback control with programmable waveform for electrical and optical stimulations. Matlab graphical user interface is used to monitor the intracranial EEG, perform the algorithm for seizure detection, and adjust the required intensity, frequency, duty cycle, and duration of electrical and optical stimulations. The whole hardware device is embedded on a printed circuit board with the size of 27.3 mm × 23.6 mm. C57BL/6 mice with Thy1-ChR2-YFP gene transfer and drug-induced seizure are used to demonstrate epileptic seizure suppression according to electrical and optogenetic stimulation in the proposed wireless EEG measurement system.

INDEX TERMS Epilepsy, wireless EEG measurement system, electrical stimulation, optical stimulation, ChR2 transgene, drug-induced seizure, open/closed-loop control, programmable stimulation waveform.

I. INTRODUCTION

Epilepsy is a kind of neurological disorder caused by abnormal discharging of brain neurons [1]. It has an incidence rate of about 0.06% and a lifetime prevalence rate of about 0.76% [2], making it a common neurological disease [3]–[5].

Therapies using electrical or optical stimulations might be the alternative solutions because ∼20%–30% of people with epilepsy remain refractory to conventional medical treatment [6] and surgeries for epilepsy-associated tissue resection are not effective for several epilepsy patients [7]. For electrical neuro-stimulation, high- (≥50 Hz) and low-frequency (0.5–5 Hz) intracranial stimulations are used to suppress epileptic seizure in animal studies [8]–[10] and patient clinical trials [11], [12]. Taking deep brain stimulation as an example, high-frequency stimulation can desynchronize focal and large-scale epileptic networks [13], whereas low-frequency stimulation can induce long-lasting hyperpolarization for seizure reduction [14] and decrease the discharges of interictal spiking [15].

Optical stimulation with implantation of opto-gene cells in the brain has also been tested for epileptic seizure suppression in recent years [16]. Under the illumination of light, excitatory opsins such as Channelrhodopsin2 (ChR2) in transgenic cells can open a cation conductance. This response can depolarize neurons and facilitate action potential generation,

The associate editor coordinating the review of this manuscript and approving it for publication was Kin Fong Lei.

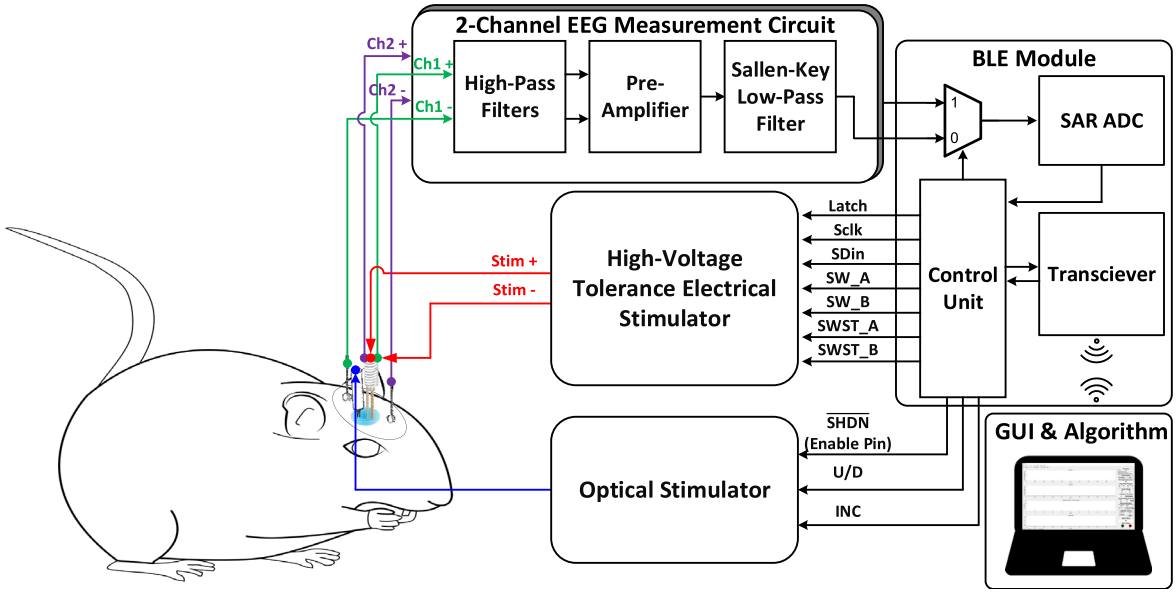

FIGURE 1. Block diagram of the proposed system.

which can suppress seizure for certain types of epilepsy [17]. Unlike electrical stimulation that affects a large area of tissues, optical stimulation only forces transgenic neurons to release neurotransmitters and does not affect normal neurons during stimulation, that is, optical stimulation can provide more precise means of brain stimulation and cause less damage than electrical stimulation on nervous tissues. Furthermore, the artifacts on the measured electroencephalography (EEG) signals induced by optical stimulation are less than those caused by electrical stimulation. Both advantages of optical stimulation over electrical stimulation have been proven by our previous work [18]. Nevertheless, potential drawbacks of optical stimulation are the requirement of transgenic cells in the brain, larger power consumption than electrical stimulation, and the issue of heat deposited in tissue [19].

Based on the above discussion, combining electrical and optogenetic stimulation in one system seems reasonable [19]. The circuits for brain signal sensing should also be applied to measure the EEG signals for verifying the effectiveness of the stimulations. Most previous works contain one or two functions among the three features, namely, electrical stimulation, optical stimulation, and EEG recording. [20] and [21] contain electrical recording and optical stimulation, whereas [10] implements electrical stimulation and electrical recording. [22] presents an arbitrary-waveform electro–optical stimulator with load-adaptive supply controller and wireless power/data communication implemented on the printed circuit board (PCB). Similar to [22], [23] implements electrical and optical stimulators. In addition to the stimulators and the EEG sensing circuit, an algorithm is needed for the recognition of epileptic seizure if closed-loop stimulation is applied. The graphical user interface (GUI) is also required for the adjustment of parameters for electrical and optical stimulations, and control of stimulation when performing open-loop stimulation. Furthermore, off-the-shelf discrete components are more accessible to construct a system for epilepsy detection and suppression. Nevertheless, the system for epilepsy containing the mentioned optical and electrical stimulations, EEG signal sensing, epileptic waveform recognition, and GUI using discrete components with accessible firmware and software has not yet been proposed. To fulfill the challenging requirements, a system including the above functions on a 27.3 mm $\times$ 23.6 mm double-layer PCB is presented in this paper. Compared with the previous work [18], this paper overcomes the drawbacks in [18] including low-output stimulated voltage less than 3.3 V, higher power consumption because of using sigma–delta analog-to-digital converter (ADC), low epileptic seizure identification without detection window in artificial intelligence (AI) algorithm, and low gain with 27 dB in the analog front-end that is insufficient for EEG signal acquisition. The proposed system in Figure 1 can provide 20 V output stimulated voltage in an animal study, a 12-bit successive approximation register (SAR) ADC is used for the benefits of low power and multichannel EEG signal acquisition, a detection window after classification is employed to enhance the accuracy of epileptic seizure detection, and an amplifier with gain of 1000 is used to improve the acquisition ability of low EEG signal.

The rest of the paper is organized as follows. Section II introduces the proposed system architecture and its operation. Section III describes the detailed implementation of each functional block, including the GUI and the AI algorithm with data processing realized by software codes. Section IV demonstrates the operation and measurement results of the proposed system on C57BL/6 mice with Thy-ChR2-YFP gene transfer. Section V concludes the features and contributions of this work.

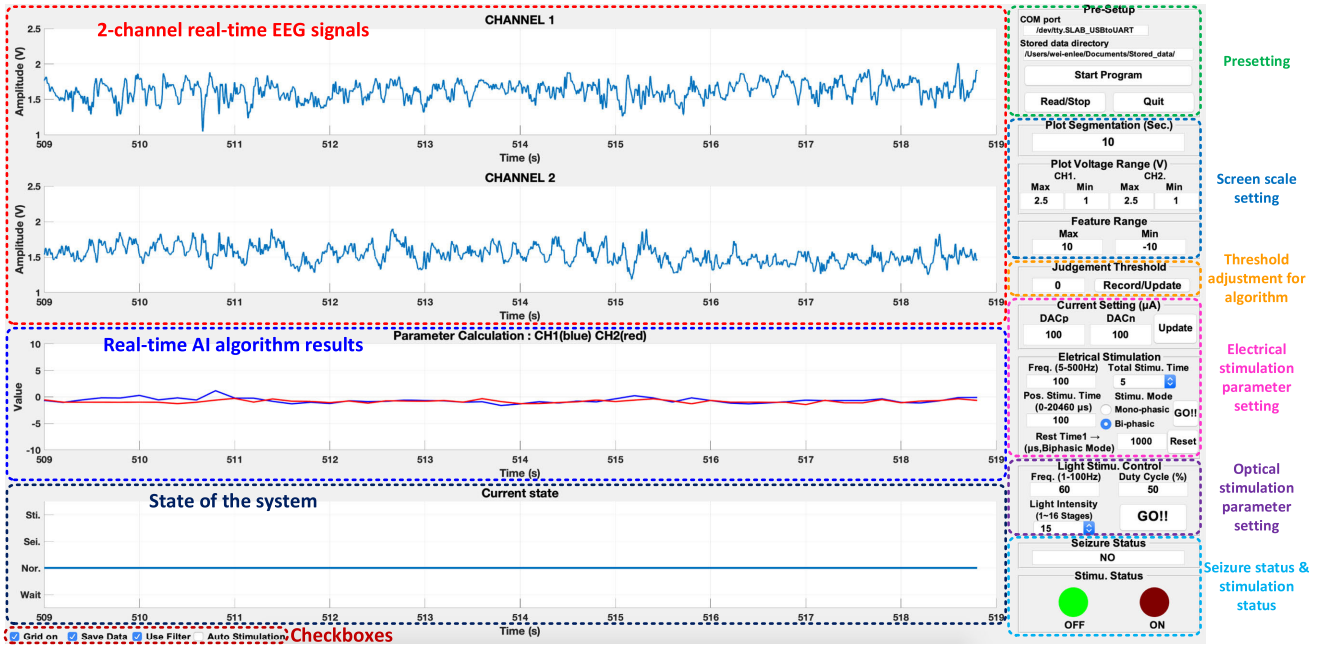

FIGURE 2. Matlab GUI for the proposed system. Left side: EEG signals, algorithm results, and state of the system. Right side: Settings for the screens, parameter adjustments for electrical and optical stimulations, and the data directory and USB dongle COM port setting.

II. SYSTEM ARCHITECTURE

Figure 1 shows the block diagram of the proposed system. The system is composed of a two-channel analog-front circuit (AFE) for EEG acquisition, optical stimulator, one-channel electrical stimulator, and a module for Bluetooth low energy (BLE) wireless data transmission. The custom GUI and the algorithm are implemented on a laptop using Matlab codes. The system on PCB is supplied by 3.8 V 60 mAh lithium battery and mounted on the head of a transgenic mouse.

The system operation is described as follows. The two-channel AFE circuit records the intracranial electroencephalography (iEEG) signals from the left and right brain of the mouse. These signals are converted into digital data by the 12-bit SAR ADC in the BLE module. The digital data are then transmitted in Bluetooth wireless communication, which is received by the Bluetooth USB dongle on the laptop and processed by the AI algorithm using Matlab codes for epileptic seizure identification. If the operation is switched to closed-loop mode on the GUI, then the electrical or optical stimulation will be performed automatically when the seizure is detected, which is beneficial for long-term monitoring. If the system is switched to open-loop mode for the on-site animal clinical trial, then the stimulation will be performed manually instead.

Figure 2 displays the custom GUI with different functions marked on the interface. Four screens on the left of the interface exhibit the real-time data of the system. The top two screens display the real-time iEEG signals from the two sensing channels, whereas the third screen shows the real-time results of the AI algorithm after linear least squares (LLS) method. The last screen is the current state of the system, which can be classified into four conditions, namely, normal state, seizure without stimulation, stimulation execution, and idle time after stimulation. For the right area of the GUI, assigning a directory for data saving and scale setting for the left four screens can be performed. Parameters of frequency, amplitude, total stimulation time, and waveform shape can also be adjusted for the electrical stimulation. Frequency, duty cycle, and intensity of the optical stimulation can also be set through this interface. With the checkboxes in the left-bottom corner, the user can enable data saving, allow digital filtering in Matlab for the display of two-channel EEG signals, and switch the mode of the system between closed- and open-loop control. By utilizing the functions on the GUI, the user can record the iEEG signals while performing customized optical or electrical stimulation and epileptic seizure recognition simultaneously.

III. SYSTEM IMPLEMENTATION

A. TWO-CHANNEL ANALOG-FRONT-END CIRCUIT

Figure 3 shows the schematic of one channel of the two-channel AFE circuit for iEEG signal measurement. A low-dropout (LDO) regulator LT1761ES5-3.3TRMPBF is used to convert the 3.8 V battery voltage into the 3.3 V power supply. The AFE circuit is composed of RC high-pass circuits, a preamplifier, and a Sallen–Key low-pass filter for each channel. The high-pass corner of the RC filter preceding the preamplifier is set around 0.05 Hz to remove the DC component of the input iEEG signal. The instrumentation amplifier AD8237 is selected as the preamplifier with 200 V/V signal gain. AD8607, which contains two micro power rail-to-rail input and output amplifiers, is used as the active component of the Sallen–Key low-pass filter with a

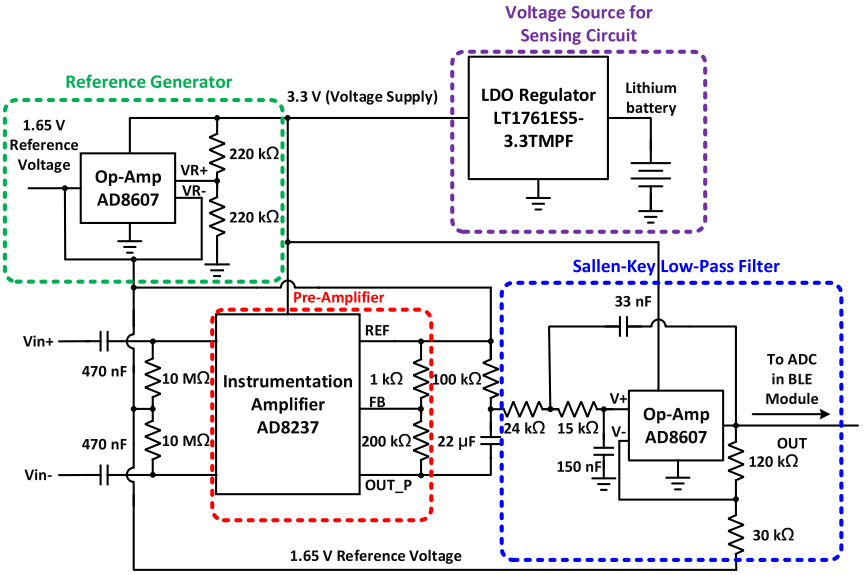

FIGURE 3. Schematic of the one-channel AFE circuit with the values specified on capacitors and resistors.

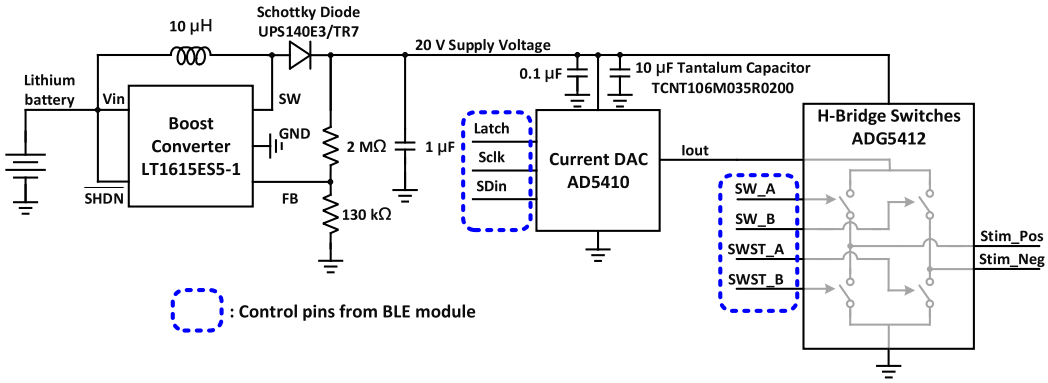

FIGURE 4. Schematic of the high-voltage electrical stimulator with the values specified on capacitors and resistors.

gain of 5. The other amplifier is used to generate the 1.65 V reference voltage for the AFE circuit. The corner of the low-pass filter is set at 120 Hz to filter the high-frequency noise and the harmonic tones of 60 Hz noise. In addition, the output of the preamplifier is ac-coupled to the Sallen–Key low-pass filter. The output signals of the Sallen–Key low-pass filters in two channels are then converted into digital data by the SAR ADC in the BLE module.

B. ELECTRICAL STIMULATION

Figure 4 illustrates that the electrical stimulator consists of one boost converter, one current digital-to-analog converter (DAC), and four switches in the H-bridge structure. The amplitude, frequency, duration, and duty cycle of the stimulation are all adjustable with the BLE module control on the stimulator. Boost converter LT1615ES5-1#TRMPBF is used to convert the supply from the battery into a 20 V supply for the current DAC and switches, which can avoid voltage saturation for 1 ms stimulation under 1 mA current with the impedance model derived from [18]. AD5410 is selected for the DAC structure because it can offer programmable current source output from 0 mA to 20 mA with a 12-bit resolution, which covers the current intensity in previous studies [8], [13]–[15]. An ADG5412 IC with four switches in a single element is selected to construct the H-bridge structure. Employing the H-bridge structure can reduce the number of DACs to one and perform well phase match that is suitable for charge-balanced stimulus. Figure 5 shows that the electrical stimulator of this system can support either monophasic or biphasic waveform with different duty cycles, frequencies, and durations via GUI control. The range of the frequency is from 5 Hz to 500 Hz, which covers the frequency of high- and low-frequency stimulation for suppressing epileptic seizure. The minimum time for each phase in both modes is 20 μs, which is limited by the BLE module CYBLE-022001-00. The developed prototype with programmable parameters on GUI provides flexibility for researchers in clinical trial including animal and human studies.

C. OPTICAL STIMULATION

Figure 6 depicts the schematic of the optical stimulator. The circuit mainly consists of an LDO regulator, a boost converter,

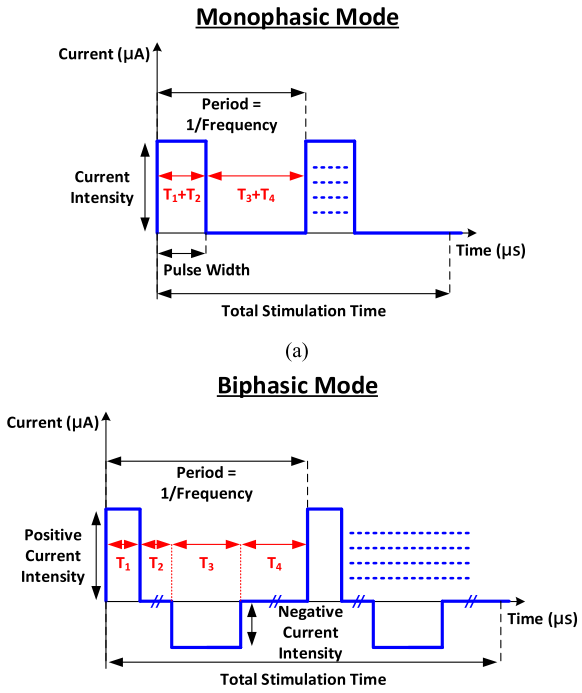

Electrical Stimulation Data format: T_1&T_3: 10 bits, T_2&T_4: 24 bits, Intensity: 8 bits, Total Stimulation Time: 0.25~6.25 s

FIGURE 5. Stimulation patterns of the proposed electrical stimulator. (a) Monophasic mode. (b) Biphasic mode.

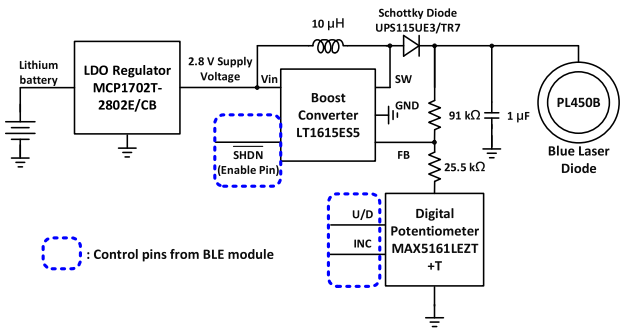

FIGURE 6. Schematic of the optical stimulator with the value specified on capacitors and resistors.

a digital potentiometer, and a blue laser diode. An output voltage lower than 3.8 V battery voltage is required to prevent the glowing of blue laser diode PL 450B during the turn-off state. This goal is realized by using an LDO regulator MCP1702T-2802E/CB to convert the battery supply into 2.8 V so that the boost converter bypasses 2.8 V rather than 3.8 V to the laser diode when the boost converter is turned off. Component LT1615ES5#TRPBF with a larger output current instead of LT1615ES5-1#TRMPBF is selected as the boost converter for the optical stimulator because the blue laser diode can consume current 10 times larger than that in the electrical stimulator under higher light intensity modes. The boost converter LT1615ES5#TRPBF can be enabled or disabled by pulling $\overline{\text{SHDN}}$ pin high or low, respectively. The digital potentiometer MAX5161LEZT+T is in series with a 25.5 kΩ

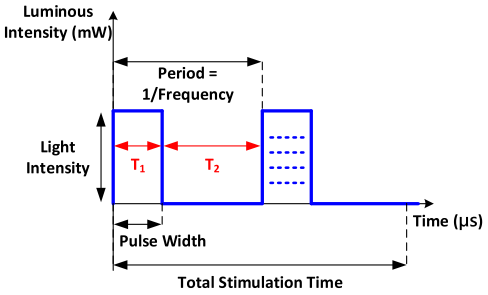

Optical Stimulation Data format: T_1&T_2: 10 bits, Intensity: 16 levels

FIGURE 7. Stimulation patterns of the proposed optical stimulator.

resistor and a 91 kΩ resistor to form the output resistors of the boost converter. Figure 7 shows the pattern for the optical stimulator. By adjusting the value of the digital potentiometer, the output voltage of the boost converter and hence the light intensity of the laser diode can be adjusted. The duty cycle of the optical stimulator and the flicker frequency $[1/(T_1+T_2)]$ can also be set. The wavelength of the blue laser diode PL 450B is 450 nm, which is suitable for usage on the mice with Thy-ChR2-YFP gene transfer for seizure suppression.

D. SOFTWARE AND FIRMWARE IMPLEMENTATION

For the implementation of data processing, AI algorithm, and GUI for controlling stimulation parameters, Matlab software is selected for its powerful functions on signal processing, data analysis, and creation of user interfaces. Although the battery, which does not introduce line noise of 60 Hz, is used as the supply of the system, the system might still receive 60 Hz interference and its harmonic tones during wireless data transmission. Thus, one moving average low-pass filter with low-pass corner frequency at 100 Hz and one direct form I infinite impulse response notch filter at 60 Hz are implemented in Matlab as digital filters to process the data from the AFE circuits further. As mentioned in Section II and shown in Figure 2, the user can select the two-channel real-time EEG signals with or without digital filtering to be displayed on the GUI. The processed data also serve as the input of the AI algorithm for epileptic seizure detection.

Figure 8 illustrates the operation of the AI algorithm, which is improved from our previous work [18] with a detection window to enhance its accuracy. The AI algorithm is described as follows. Feature extraction is first performed on the input data. The features include specific frequency tones for epileptic seizure, approximate entropy (ApEn), and the amplitude of signals. According to previous studies [18], [24], the frequency tones around 5, 10, and 15 Hz are larger in the epileptic seizure waveforms than the normal iEEG signals. Based on this observation, the sampling frequency in the SAR ADC is selected to be 1 kHz. With the interval of the discrete-time Fourier transform (DFT) set to 200, feature extraction can directly acquire the frequency tones of 5, 10, and 15 Hz by selecting the first, second, and third tones of DFT's outputs. The ApEn is adopted to quantify

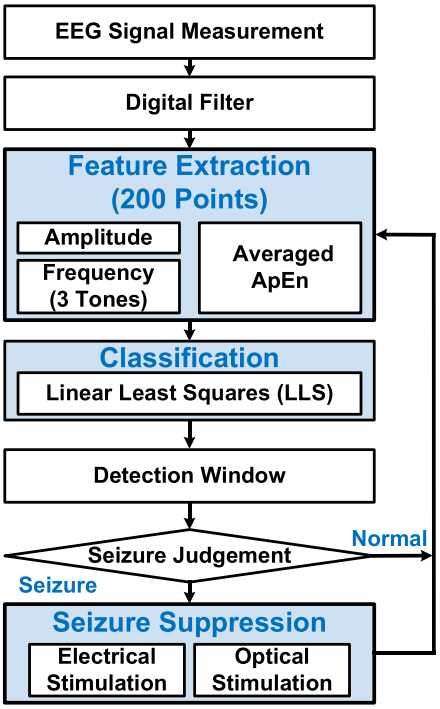

FIGURE 8. Signal flow chart for the proposed AI algorithm with data processing.

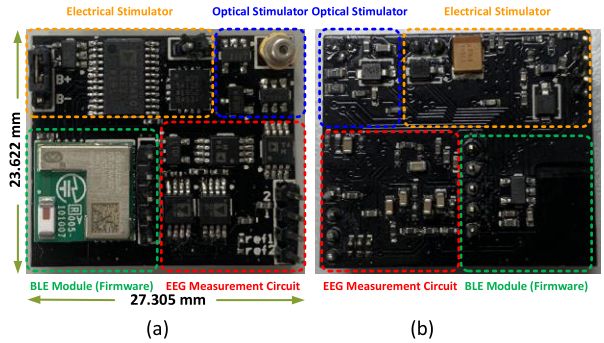

FIGURE 9. Proposed system on PCB. (a) Top view. (b) Bottom view.

the regularity of one signal [25], [26]. Repetitive iEEG signals during seizure exhibit a larger ApEn than iEEG signals in the normal state because a larger ApEn implies a higher signal regularity. The interval for ApEn calculation is also set to 200 to be consistent with the succeeding classification. Owing to a larger amplitude of iEEG signal when a seizure occurs, the amplitude of the iEEG signal is selected as the third parameter for feature extraction with its calculation interval the same as that in ApEn and DFT operations.

After feature extraction, the LLS method is applied for the classification of the processed data. Measured iEEG signal data with and without epileptic seizure are utilized to train the parameters required for classification. The results from the LLS are then used for seizure judgement by comparing the results with a specific parameter. One detection window preceding the seizure judgement is added to improve the accuracy of the algorithm further. The detection window can be adjusted to control the sensitivity of seizure detection.

TABLE 1. Off-the-shelf components in the proposed system.

Components	Relative Circuit Block	Company	Model
LDO Regulator	AFE Circuit	LT (ADI)	LT1761ES5
INA	AFE Circuit	ADI	AD8237
Op-Amp	AFE Circuit	ADI	AD8607
Boost Converter	Electrical Stimulator	LT (ADI)	LT1615ES5-1
Current DAC	Electrical Stimulator	ADI	AD5410
H-bridge Switches	Electrical Stimulator	ADI	ADG5412
LDO Regulator	Optical Stimulator	Microchip	MCP1702T
Boost Converter	Optical Stimulator	LT (ADI)	LT1615ES5
Digital Potentiometer	Optical Stimulator	Maxim	MAX5161
Blue Laser Diode	Optical Stimulator	OSRAM	PL 450B
LDO Regulator	Firmware	LT (ADI)	LT1761ES5
BLE Module	Firmware	Cypress	CYBLE

The value of the detection window is designed to be 3 to consider the tradeoff between accuracy and decision time, that is, the occurrence of a seizure is determined by three consecutive judgements. If the results from the three consecutive judgements are not the same, then the final decision will be the same as that in the previous decision.

For firmware implementation, the BLE module CYBLE-022001-00 along with an LDO regulator are used. An LDO regulator LT1761ES5-3.3TRMPBF, which is the same component used in the AFE circuit, is selected to provide a 3.3 V supply for the BLE module. As mentioned in Section II, the BLE module is employed for data transmission of iEEG signals and data reception of parameters to control the electrical and optical stimulators. A 12-bit SAR ADC in this module is utilized to convert analog signals from the outputs of two-channel AFE circuit into digital data for wireless data transmission. Table 1 summarizes the main discrete components in the proposed system on the PCB, which are beneficial for the reproduction.

IV. MEASUREMENT RESULTS

This section is divided into two parts. The first subsection presents the measurement results of the circuits of the proposed system and results of the AI algorithm on seizure recognition. The second subsection describes the setup for the in vivo experiment, including the mice used for function verification and the animal testing flow. This subsection also exhibits the experimental results of animal testing, which include the verification of seizure suppression by electrical and optical stimulators, and the comparison table with other prior architectures.

A. SYSTEM MEASUREMENT RESULTS

Figure 9 shows the top and bottom views of the realized PCB. The total area for this PCB is 27.3 mm × 23.6 mm with a weight of 2.86 g. To ensure a low interference between the circuits, the ground of PCB is divided into four parts, namely, battery ground, ground for the BLE module, ground for the stimulators, and ground for the AFE circuit, with 0402 beads connected between the battery ground and other grounds.

An 1 kΩ resistor is connected to the output of the stimulator to verify the function of the electrical stimulator. Figure 10 presents the measured voltage waveforms across the resistor under different conditions. It demonstrates that the electrical stimulator can perform high- and low-frequency stimulations.

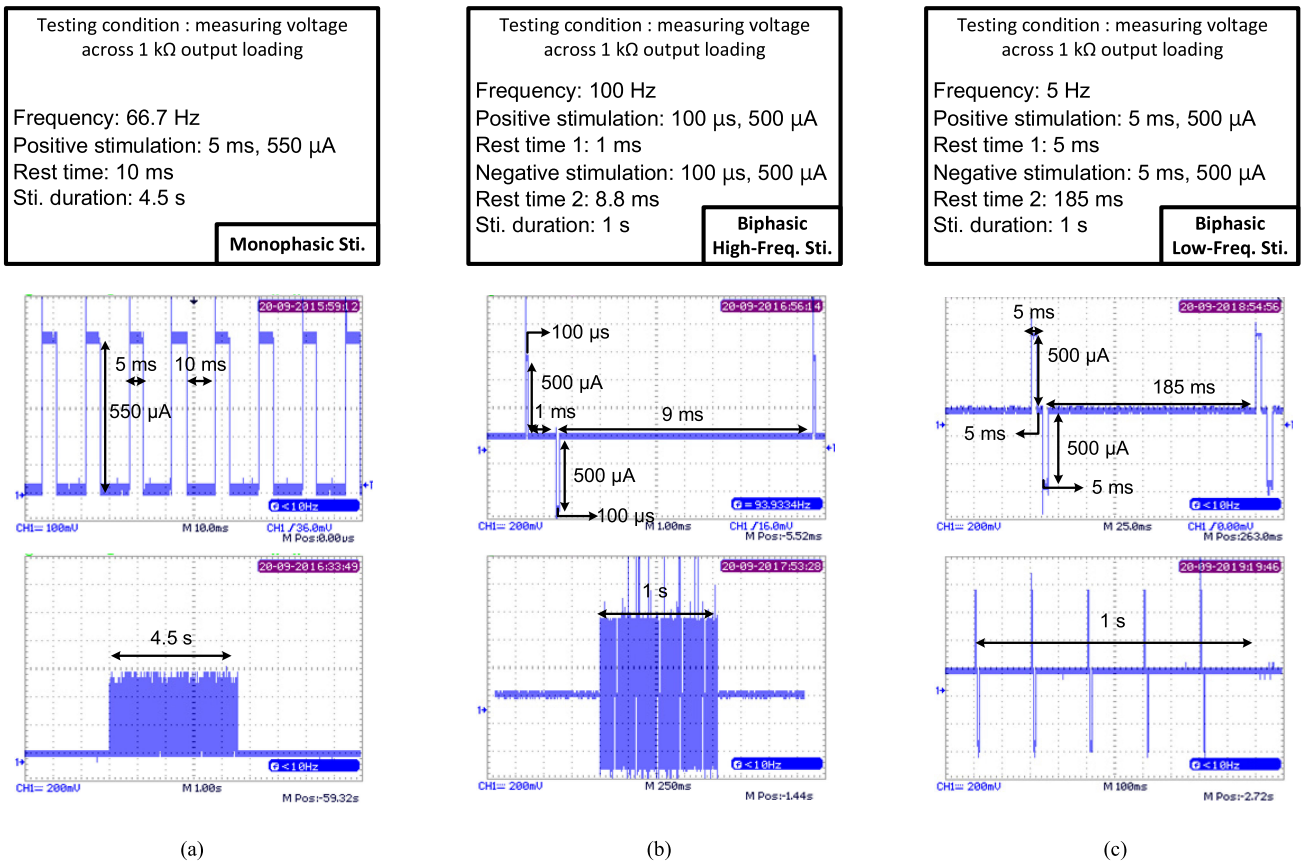

FIGURE 10. Functional tests of electrical stimulation. (a) Monophasic stimulation. (b) Biphasic high-frequency stimulation. (c) Biphasic low-frequency stimulation.

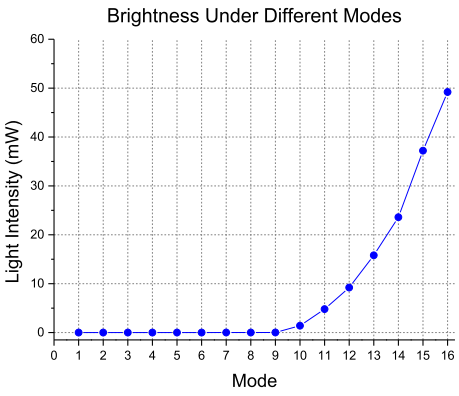

FIGURE 11. Measured result of output optical power under different intensity modes.

The stimulator can also switch between monophasic and biphasic modes. The output power of the blue laser diode of the optical stimulator under different intensity modes is also tested, which is plotted in Figure 11. Sixteen levels in the 32-tap digital potentiometer are utilized to produce 16 different light intensities from the diode.

The seizure detection algorithm is verified by application to an 1-hour dataset from the in vivo experiment with waveforms from normal state to seizure state. Figure 12 (a) shows a segment of this dataset with the detection results on the iEEG signals. Two subsegments from Figure 12 (a) in the normal state and seizure state are shown in Figures 12 (b) and 12 (c), respectively. The calculated accuracy is 98.02%, which is 9% better than our previous work [18] because of the detection window used. The calculated F1-score is 0.8011.

B. VERIFICATION OF SEIZURE SUPPRESSION WITH IN VIVO EXPERIMENTS

For the animal testing, C57BL/6 mice with Thy-ChR2-YFP gene transfer are used, which are supported by the National Cheng Kung University Hospital and National Cheng Kung University Laboratory Animal Center. Figure 13 presents the implant position of the electrodes and the gene-transferring C57BL/6 mouse with electrodes mounted on its head. The electrodes are mounted with the aid of an stereotaxic apparatus. A three-channel electrode (MS333/3-B/SPC, Plastic One) is implanted in the middle of the mouse's head, E1, with one channel at the right brain and two channels with twisted wires at the left brain. The middle channel is used for stimulation, while the side channels are connected to the inputs of the two-channel AFE circuit. E2 and E3 are two stainless-steel screws (PACK-SMIB1.2-3, MISUMI) of the mouse's head as the reference points of the AFE circuit. E4 is for optical stimulation constructed by fiber (FT200EMT, Thorlabs) with stainless steel on the outer layer.

TABLE 2. Comparison with previous works.

	TBioCAS'18 [20]	JSSC'18 [28]	TNSRE'19 [22]	TBioCAS'19 [29]	EMBC'13 [30]	Sensors'15 [31]	TBioCAS'17 [21]	This Work
Technology	0.35 μm	0.18 μm	Discrete	Discrete	Discrete	Discrete	Discrete	Discrete
Electrical Stimulation	No	Bi-phasic	Arbitrary	N/A	N/A	N/A	N/A	Mono-phasic & Bi-phasic
Optical Stimulation	Yes	N/A	Yes	N/A	Yes	Yes	Yes	Yes
No. Rec. Channels	4	16	N/A	32	1	2	32	2
Algorithm	N/A	Feature Extraction + Ridge Regression Classification	N/A	Feature Extraction + SVM Classification	N/A	N/A	Spike Detection	Feature Extraction + LLS Classification
GUI	Yes	N/A	N/A	Yes	N/A	N/A	N/A	Matlab GUI
Wireless Communication	Commercial	Custom Integrated	Custom Integrated	Commercial	Commercial	Commercial	Commercial	Commercial

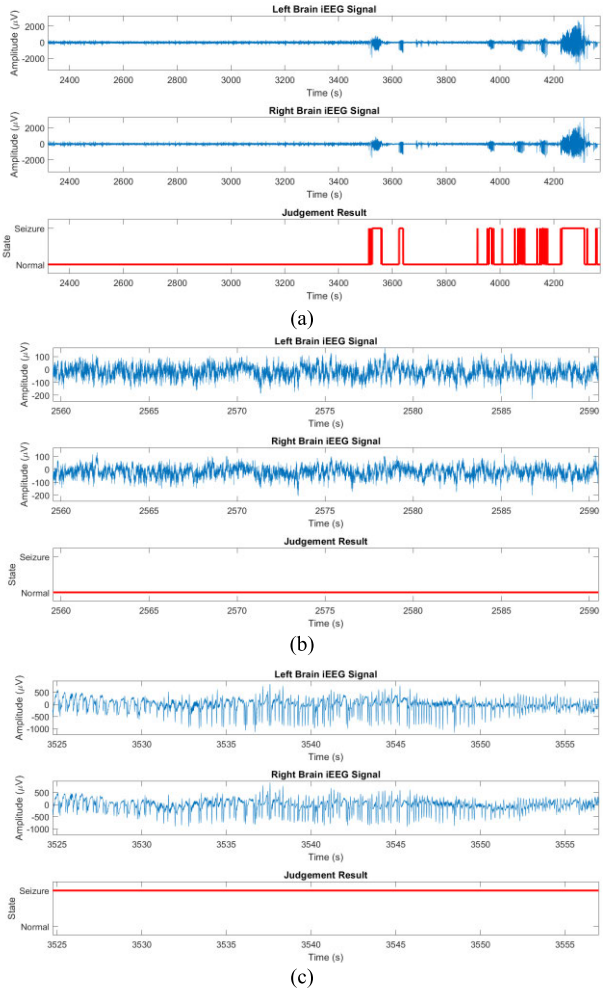

FIGURE 12. Results of the proposed algorithm. (a) From normal to seizure condition. (b) Normal condition. (c) Seizure condition.

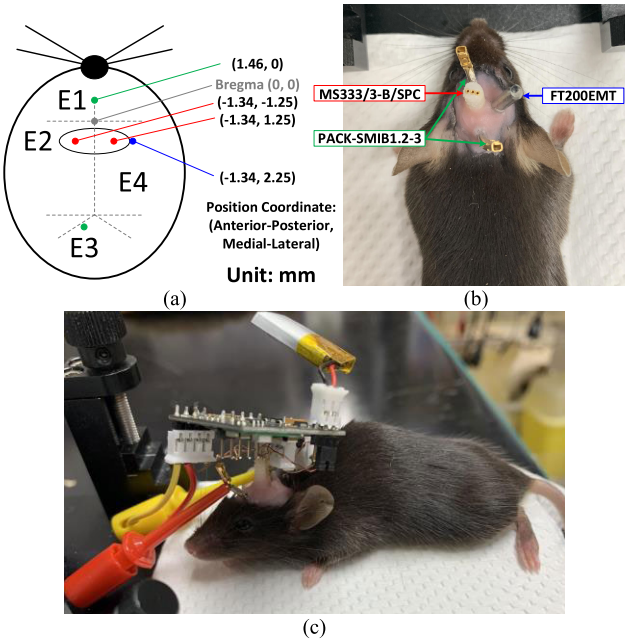

FIGURE 13. Setup for in vivo experiments. (a) Implant position of electrodes. (b) Mouse with mounted electrodes for the experiment. (c) Proposed system with PCB on mouse's head.

Figure 14 illustrates the procedure of the in vivo experiment. The mouse is first placed under anesthesia using isoflurane, with the concentration and gas flow controlled by anesthesia system (AS-01, Norvap). The mouse's weight is measured, and seizure-inducing drug such as pilocarpine or kainic acid is injected. After the induction of epileptic seizure, either electrical stimulation or optical stimulation is performed for seizure suppression.

Figure 15 shows the results of epileptic seizure suppression. The stimulation parameters are also listed at the bottom of figure. It demonstrates that the seizure is suppressed immediately after stimulation. However, settling time without iEEG recording [10], [27] is required for EEG sensing circuit after stimulation.

Figure 16 displays the results for optical stimulation on seizure suppression. The seizure is suppressed after optical stimulation. Nevertheless, no settling time is required

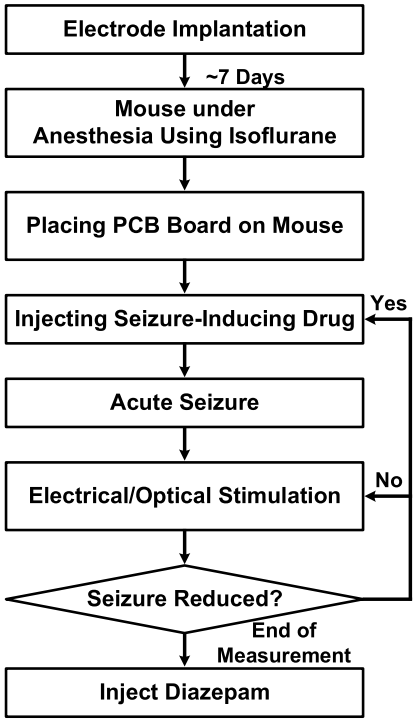

FIGURE 14. Procedure of the in vivo experiment.

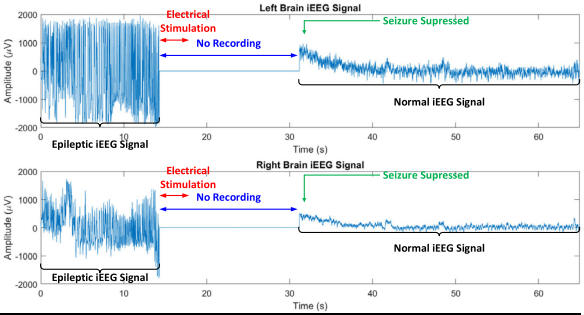

Mode	Frequency	Amplitude	Pulse Width	Total Sti. Time
Biphasic	100 Hz	100 μA (Both Phase)	100 μs	3 s

FIGURE 15. Epileptic seizure suppression by electrical stimulation with stimulation parameters.

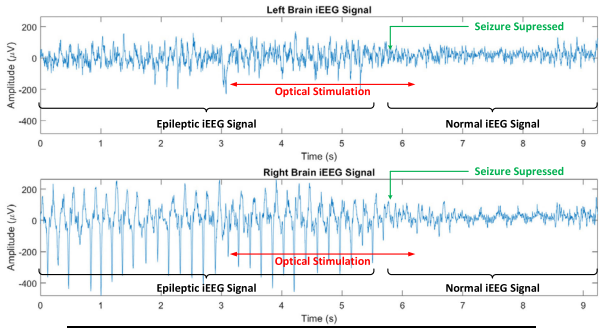

Frequency	Intensity	Duty Cycle	Total Sti. Time
60 Hz	58 mW	50%	3 s

FIGURE 16. Epileptic seizure suppression by optical stimulation with stimulation parameters.

compared with the electrical stimulation method, which is one of the advantages of optical stimulation. Table 2 summarizes the performance and features of the proposed system and previous architectures.

V. CONCLUSION

In this paper, a wireless intelligent EEG measurement system using off-the-shelf components for epilepsy detection and stimulation is proposed. Electrical and optical stimulators are implemented for the suppression of epileptic seizures. A two-channel sensing circuit and the AI algorithm are employed for iEEG monitoring and seizure identification. A GUI is provided for stimulation parameter adjustment, open- and closed-loop control, and real-time iEEG waveform display. The discrete components of the proposed system are integrated on a 27.3 mm × 23.6 mm PCB, which can be mounted directly on the head of a C57BL/6 mouse with Thy-ChR2-YFP gene transfer. The proposed system and methods are useful for researchers to study in the clinical trial and design of integrated circuits and systems.

REFERENCES

[1] A. H. Ropper, M. A. Samuels, J. P. Klein, and S. Prasad, *Adams and Victor's Principles of Neurology*, 10th ed. New York, NY, USA: McGraw-Hill, 2014.

[2] E. Beghi, "The epidemiology of epilepsy," *Neuroepidemiology*, vol. 54, no. 2, pp. 185–191, Mar. 2020.

[3] K. M. Fiest, K. M. Sauro, S. Wiebe, S. B. Patten, C.-S. Kwon, J. Dykeman, T. Pringsheim, D. L. Lorenzetti, and N. Jetté, "Prevalence and incidence of epilepsy: A systematic review and meta-analysis of international studies," *Neurology*, vol. 88, no. 3, pp. 296–303, Jan. 2017.

[4] E. Trinka, P. Kwan, B. Lee, and A. Dash, "Epilepsy in Asia: Disease burden, management barriers, and challenges," *Epilepsia*, vol. 60, pp. 7–21, Mar. 2019.

[5] E. Beghi, G. Giussani, E. Nichols, F. Abd-Allah, J. Abdela, A. Abdelalim, H. N. Abraha, M. G. Adib, S. Agrawal, F. Alahdab, and A. Awasthi, "Global, regional, and national burden of epilepsy, 1990–2016: A systematic analysis for the global burden of disease study 2016," *Lancet Neurol.*, vol. 18, no. 4, pp. 357–375, Apr. 2019.

[6] L. Dalic and M. Cook, "Managing drug-resistant epilepsy: Challenges and solutions," *Neuropsychiatric Disease Treat.*, vol. 12, pp. 2605–2616, Oct. 2016.

[7] M. Mohan, S. Keller, A. Nicolson, S. Biswas, D. Smith, J. O. Farah, P. Eldridge, and U. Wieshmann, "The long-term outcomes of epilepsy surgery," *PLoS ONE*, vol. 13, no. 5, May 2018, Art. no. e0196274.

[8] P. Rajdev, M. Ward, and P. Irazoqui, "Effect of stimulus parameters in the treatment of seizures by electrical stimulation in the kainate animal model," *Int. J. Neural Syst.*, vol. 21, no. 2, pp. 151–162, Apr. 2011.

[9] H. Khosravani, P. L. Carlen, and J. L. P. Velazquez, "The control of seizure-like activity in the rat hippocampal slice," *Biophys. J.*, vol. 84, no. 1, pp. 687–695, Jan. 2003.

[10] M. T. Salam, J. L. P. Velazquez, and R. Genov, "Seizure suppression efficacy of closed-loop versus open-loop deep brain stimulation in a rodent model of epilepsy," *IEEE Trans. Neural Syst. Rehabil. Eng.*, vol. 24, no. 6, pp. 710–719, Jun. 2016.

[11] F. T. Sun and M. J. Morrell, "The RNS system: Responsive cortical stimulation for the treatment of refractory partial epilepsy," *Expert Rev. Med. Devices*, vol. 11, no. 6, pp. 563–572, Nov. 2014.

[12] K. Starnes, K. Miller, L. Wong-Kisiel, and B. N. Lundstrom, "A review of neurostimulation for epilepsy in pediatrics," *Brain Sci.*, vol. 9, no. 10, p. 283, Oct. 2019.

[13] T. Yu, X. Wang, Y. Li, G. Zhang, G. Worrell, P. Chauvel, D. Ni, L. Qiao, C. Liu, L. Li, L. Ren, and Y. Wang, "High-frequency stimulation of anterior nucleus of thalamus desynchronizes epileptic network in humans," *Brain*, vol. 141, pp. 2631–2643, Jul. 2018.

[14] S. Toprani and D. M. Durand, "Long-lasting hyperpolarization underlies seizure reduction by low frequency deep brain electrical stimulation," *J. Physiol.*, vol. 591, no. 22, pp. 5765–5790, Nov. 2013.

[15] J. Yamamoto, A. Ikeda, T. Satow, K. Takeshita, M. Takayama, M. Matsuhashi, R. Matsumoto, S. Ohara, N. Mikuni, J. Takahashi, S. Miyamoto, W. Taki, N. Hashimoto, J. C. Rothwell, and H. Shibasaki, "Low-frequency electric cortical stimulation has an inhibitory effect on epileptic focus in mesial temporal lobe epilepsy," *Epilepsia*, vol. 43, no. 5, pp. 491–495, May 2002.

[16] J. T. Paz and J. R. Huguenard, "Optogenetics and epilepsy: Past, present and future," *Epilepsy Currents*, vol. 15, no. 1, pp. 34–38, Jan. 2015.

[17] M. C. Walker and D. M. Kullmann, "Optogenetic and chemogenetic therapies for epilepsy," *Neuropharmacology*, vol. 168, May 2020, Art. no. 107751.

[18] S.-Y. Lee, C. Tsou, Z.-X. Liao, P.-H. Cheng, P.-W. Huang, H.-Y. Lee, C.-C. Lin, and G.-S. Shieh, "A programmable EEG monitoring SoC with optical and electrical stimulation for epilepsy control," *IEEE Access*, vol. 8, pp. 92196–92211, May 2020.

[19] A. C. Thompson, P. R. Stoddart, and E. D. Jansen, "Optical stimulation of neurons," *Current Mol. Imag.*, vol. 3, no. 2, pp. 162–177, Feb. 2015.

[20] R. Ramezani, A. Jackson, T. G. Constandinou, P. Degenaar, Y. Liu, F. Dehkhoda, A. Soltan, D. Haci, H. Zhao, D. Firfilionis, A. Hazra, and M. O. Cunningham, "On-probe neural interface ASIC for combined electrical recording and optogenetic stimulation," *IEEE Trans. Biomed. Circuits Syst.*, vol. 12, no. 3, pp. 576–588, Jun. 2018.

[21] G. Gagnon-Turcotte, Y. LeChasseur, C. Bories, Y. Messaddeq, Y. De Koninck, and B. Gosselin, "A wireless headstage for combined optogenetics and multichannel electrophysiological recording," *IEEE Trans. Biomed. Circuits Syst.*, vol. 11, no. 1, pp. 1–14, Feb. 2017.

[22] H. Kassiri, F. D. Chen, M. T. Salam, M. Chang, B. Vatankhahghadim, P. Carlen, T. A. Valiante, and R. Genov, "Arbitrary-waveform electro-optical intracranial neurostimulator with load-adaptive high-voltage compliance," *IEEE Trans. Neural Syst. Rehabil. Eng.*, vol. 27, no. 4, pp. 582–593, Apr. 2019.

[23] Y. Jia and M. Ghovanloo, "Towards a mm-sized free-floating wireless implantable opto-electro stimulation device," in *Proc. IEEE Biomed. Circuits Syst. Conf. (BioCAS)*, Oct. 2019, pp. 1–4.

[24] C.-P. Young, S.-F. Liang, D.-W. Chang, Y.-C. Liao, F.-Z. Shaw, and C.-H. Hsieh, "A portable wireless online closed-loop seizure controller in freely moving rats," *IEEE Trans. Instrum. Meas.*, vol. 60, no. 2, pp. 513–521, Feb. 2011.

[25] V. Srinivasan, C. Eswaran, and N. Sriraam, "Approximate entropy-based epileptic EEG detection using artificial neural networks," *IEEE Trans. Inf. Technol. Biomed.*, vol. 11, no. 3, pp. 288–295, May 2007.

[26] M. S. Akter, M. R. Islam, Y. Iimura, H. Sugano, K. Fukumori, D. Wang, T. Tanaka, and A. Cichocki, "Multiband entropy-based feature-extraction method for automatic identification of epileptic focus based on high-frequency components in interictal iEEG," *Sci. Rep.*, vol. 10, no. 1, pp. 1–17, Apr. 2020, doi: 10.1038/s41598-020-62967-z.

[27] A. Bagheri, S. R. I. Gabran, M. T. Salam, J. L. P. Velazquez, R. R. Mansour, M. M. A. Salama, and R. Genov, "Massively-parallel neuromonitoring and neurostimulation rodent headset with nanotextured flexible microelectrodes," *IEEE Trans. Biomed. Circuits Syst.*, vol. 7, no. 5, pp. 601–609, Oct. 2013.

[28] C.-H. Cheng, P.-Y. Tsai, T.-Y. Yang, W.-H. Cheng, T.-Y. Yen, Z. Luo, X.-H. Qian, Z.-X. Chen, T.-H. Lin, W.-H. Chen, W.-M. Chen, S.-F. Liang, F.-Z. Shaw, C.-S. Chang, Y.-L. Hsin, C.-Y. Lee, M.-D. Ker, and C.-Y. Wu, "A fully integrated 16-channel closed-loop neural-prosthetic CMOS SoC with wireless power and bidirectional data telemetry for real-time efficient human epileptic seizure control," *IEEE J. Solid-State Circuits*, vol. 53, no. 11, pp. 3314–3326, Nov. 2018.

[29] T. Zhan, S. Z. Fatmi, S. Guraya, and H. Kassiri, "A resource-optimized VLSI implementation of a patient-specific seizure detection algorithm on a custom-made 2.2 cm^2 wireless device for ambulatory epilepsy diagnostics," *IEEE Trans. Biomed. Circuits Syst.*, vol. 13, no. 6, pp. 1175–1185, Dec. 2019.

[30] R. Ameli, A. Mirbozorgi, J.-L. Neron, Y. LeChasseur, and B. Gosselin, "A wireless and batteryless neural headstage with optical stimulation and electrophysiological recording," in *Proc. 35th Annu. Int. Conf. IEEE Eng. Med. Biol. Soc. (EMBC)*, Jul. 2013, pp. 5662–5665.

[31] G. Gagnon-Turcotte, A. Kisomi, R. Ameli, C.-O. Camaro, Y. LeChasseur, J.-L. Néron, P. Bareil, P. Fortier, C. Bories, Y. de Koninck, and B. Gosselin, "A wireless optogenetic headstage with multichannel electrophysiological recording capability," *Sensors*, vol. 15, no. 9, pp. 22776–22797, Sep. 2015.

WEI-EN LEE (Member, IEEE) was born in Taichung, Taiwan, in 1996. He received the B.S. degree in electrical engineering from the National Taiwan University, Taipei, Taiwan, in 2018, where he is currently pursuing the M.S. degree with the Graduate Institute of Electronics Engineering. His research interests include analog-front-end IC design, power management circuit, and system design for epilepsy control.

CHIEH TSOU (Member, IEEE) was born in Kaohsiung, Taiwan, in 1992. He received the B.S. degree in electrical engineering from the National Cheng Kung University, Tainan, Taiwan, in 2014, where he is currently pursuing the Ph.D. degree in electrical engineering. His research interests include the design of baseband modulation ASIC, MCU with peripheral interface, memory verification, decimation filter, bio-signal detection algorithm with hardware design, SOC integration, software design, firmware design, biomedical system platform setup and PCB design, and animal testing. His awards and accepted papers include excellent work in 2014 cell-based digital circuit design held by CIC, Taiwan, and in 2015, Silicon Awards held by Macronix, Taiwan. He attended the 2015 ISBB, 2019 ISSCC, and 2019 AICAS.

ZHAN-XIAN LIAO (Graduate Student Member, IEEE) was born in Kaohsiung, Taiwan, in 1995. He received the B.S. degree from the National Cheng Kung University, Taiwan, in 2017, where he is currently pursuing the Ph.D. degree with the Department of Electrical Engineering.

His research interest includes power management IC design.

PO-YEN LU was born in Taoyuan, Taiwan, in 1996. He received the B.S. degree in mechanical and mechatronic engineering from the National Taiwan Ocean University, Keelung, Taiwan, in 2018, and the M.S. degree in mechanical engineering from the National Cheng Kung University, Tainan, Taiwan, in 2021. His research interests include epilepsy animal model estimation and optogenetic stimulation experiments on mice's brains for seizure suppression.

TSUNG-HSIEN LIN (Senior Member, IEEE) received the B.S. degree in electronics engineering from the National Chiao Tung University, Hsinchu, Taiwan, and the M.S. and Ph.D. degrees in electrical engineering from the University of California at Los Angeles, Los Angeles, CA, USA, in 1997 and 2001, respectively. In 2000, he joined Broadcom Corporation, Irvine, CA, where he was a Senior Staff Scientist and involved in wireless transceiver (TRX) developments. In 2004, he joined the Graduate Institute of Electronics Engineering and the Department of Electrical Engineering, National Taiwan University, Taipei, Taiwan, where he is currently a Professor. His current research interests include the design of wireless TRXs, clock and frequency generation systems, delta–sigma modulators, and sensor interface circuits. He served as a Technical Program Committee (TPC) Member for the IEEE Asian Solid-State Circuit Conference (A-SSCC), from 2005 to 2011, and an International Technical Program Committee Member for the ISSCC, from 2010 to 2016. He was a recipient of the Best Presentation Award for his paper presented at the 2007 IEEE VLSI-DAT Symposium and a co-recipient of the Best Paper Award at the IEEE VLSI-DAT Symposium, in 2015. He was the TPC Vice-Chair of 2011 A-SSCC and the TPC Chair of 2017 A-SSCC. He was the Far-East Regional Committee Chair of 2016 ISSCC. He served as the TPC Chair and the General Chair for 2020 and 2021 VLSI-DAT Symposium, respectively. He was a Guest Editor of the IEEE JOURNAL OF SOLID-STATE CIRCUITS (JSSC), in 2012 and 2018. He was an Associate Editor of JSSC, from 2013 to 2015.

SHUENN-YUH LEE (Senior Member, IEEE) was born in Taichung, Taiwan, in 1966. He received the B.S. degree from the National Taiwan Ocean University, Keelung, Taiwan, in 1988, and the M.S. and Ph.D. degrees from the National Cheng Kung University, Tainan, Taiwan, in 1994 and 1999, respectively.

He is currently a Professor with the Department of Electrical Engineering, National Cheng Kung University. His current research interests include the design of analog and mixed-signal integrated circuits, biomedical circuits and systems, low-power and low-voltage analog circuits, and RF front-end integrated circuits for wireless communications.

Dr. Lee is a member of the Circuits and Systems (CAS) Society, the Solid-State Circuits Society, and the Medicine and Biology Society of IEEE. He is also a member of IEICE. He served as the Technical Program Chair (TPC) for the 2014/2015 International Symposium on Bioelectronics and Bioinformatics (ISBB) and the 2015 Taiwan and Japan Conference on Circuits and Systems (TJCAS). From 2013 to 2016, he served as the Chairman for IEEE Solid-State Circuits Society Tainan Chapter. From 2016 to 2017, he served as the Vice Chairman for IEEE Tainan Section. Since 2016, he has been serving as an Associate Editor for IEEE TRANSACTION ON BIOMEDICAL CIRCUITS AND SYSTEMS.

CHOU-CHING K. LIN (Senior Member, IEEE) received the bachelor's degree in medicine from the National Yang-Ming University, Taipei, Taiwan, in 1988, and the M.Sc. and Ph.D. degrees in biomedical engineering from Case Western Reserve University, Cleveland, OH, USA, in 1994 and 1997, respectively. He is currently a Professor and the Chairman of the Department of Neurology and an Adjunct Professor with the Department of Biomedical Engineering, National Cheng Kung University, Tainan, Taiwan. His areas of interest include functional MRI, brain–computer interface (BCI), brain stimulation, and neural network modeling.

GIA-SHING SHIEH was born in Kaohsiung, Taiwan, in 1965. He received the M.D. degree from China Medical University, Taichung, Taiwan, in 1991, and the Ph.D. degree from the National Cheng Kung University, Tainan, Taiwan, in 2006.

He is currently an Associate Professor with the Department of Urology, National Cheng Kung University Medical College, Tainan. He is also an Associate Professor with the Department of Biochemistry and Molecular Biology, National Cheng Kung University Medical College. His studies involve gene therapy, viral delivery systems, oncology, and immunology.